6-4-2001

Use of short-pulse laser for optical tomography of tissues

Kunal Mitra

Tuan Vo-Dinh

PROCEEDINGS OF SPIE

SPIEDigitalLibrary.org/conference-proceedings-of-spie

Use of short-pulse laser for optical tomography of tissues

Kunal Mitra
Tuan Vo-Dinh

SPIE.

Use of Short-Pulse Laser For Optical Tomography of Tissues

Kunal Mitra*[a] and Tuan Vo-Dinh**[b]

[a] Florida Institute of Technology, Melbourne, FL 32901
[b] Oak Ridge National Laboratory, Oak Ridge, TN 37831

ABSTRACT

This paper analyzes the short pulse laser propagation through tissues for development of a time-resolved optical tomography system for detection of tumors and inhomogeneities in tissues. Traditional method for analyzing optical transport in tissues is the parabolic or diffusion approximation in which the energy flux is assumed proportional to the fluence (intensity averaged over all solid angles) gradients. The inherent drawback in this model is that it predicts infinite speed of propagation of the optical signal. In this paper accurate hyperbolic or wave nature of transient radiative transfer formulation is used to overcome such drawbacks. The transmitted and reflected intensity distributions are obtained using hyperbolic P_1 and discrete ordinates method and the results are compared with the parabolic diffusion P_1 approximation. Parametric study of tissue thickness, pulse width, scattering and absorption coefficients of tissues, tumor location, size and properties, and scattering phase function distribution is also performed to analyze their effect on the transmitted and reflected optical signals.

Keywords: short pulse laser, transient radiative transfer, tissues

1. INTRODUCTION

Time-resolved optical tomography is an example of short-pulse laser interactions with scattering and absorbing media such as biological tissues, which is of great scientific and engineering interest.[1,2,3,4,5,6,7] The nascent field of optical tomography for medical imaging is made possible by a spectral window in the visible and infrared wavelength region where light absorption is very small and scattering dominates.[1,2] Optical methods are a recent addition to the arsenal of non-invasive diagnostic tools available for the detection of disease, such as x-ray computed tomography, magnetic resonance imaging, positron emission tomography, single photon emission computed tomography, ultrasound imaging, and electrical impedance tomography. In optical tomography a short pulse laser is focused on the region to be probed and the time dependent scattered fluence rates are measured at different locations using ultrafast detectors. It is the intent of the method to obtain information about the interior of the tissue medium non-invasively from the time-resolved fluence or intensity measurements. But before the development of the inverse algorithm it is critical to develop accurate forward transient radiative transfer models, which will match the experimental results.

Short pulse probing techniques have distinct advantages over conventional very large pulse width or cw lasers primarily due to the additional information conveyed about tissue interior by the temporal variation of the observed signal. When conventional cw laser sources are utilized the information available is the magnitude of the net attenuation and the angular distribution of the transmitted or reflected signal. The scattered, reflected, and transmitted signals measured when short pulse lasers interact with scattering-absorbing media like tissues possess a unique feature compared to the steady state or cw laser measurements. The distinct feature is the multiple scattering induced temporal signature that persists for time periods greater than the duration of the source pulse and is a function of the source pulse width, the scattering and absorbing properties of the medium, and the location in the medium where the properties undergo changes. If the detection is carried out at the same short time scale (comparable to the order of the pulse width), the signal continues to be observed even at large times after the pulse has been off due to the time taken for the photons to migrate to the detector after multiple scattering in the media. Moreover, steady state measurements are somewhat cumbersome because they require several independent measurements at different

* kmitra@fit.edu; 150 W. University Blvd., Melbourne, FL 32901; phone: (321) 674 7131; fax: (321) 674 8813
** vodinht@ornl.gov; P.O. Box 2008, M.S. 6101, Oak Ridge, TN 37831-6101; phone: (865) 574 6249; fax: (865) 576 7651

Biomedical Diagnostic, Guidance, and Surgical-Assist Systems III, Tuan Vo-Dinh, Warren S. Grundfest, David A. Benaron, Editors, Proceedings of SPIE Vol. 4254 (2001) © 2001 SPIE · 1605-7422/01/$15.00

source-detector spacing to yield the optical properties of interest. Another technique that is commonly used for biomedical imaging is to collect the ballistic or snake-like photons by an appropriate gating technique. But tracking these ballistic photons may not be of practical use for thicker tissue samples.[1]

Most previous studies have considered the parabolic diffusion approximation,[1,4-7,8,9,10] which is derived from the complete transport equation by neglecting certain time derivative terms from radiative transport equation, except a brief discussion by one researcher.[11] Some of the studies cited have experimentally investigated short pulse laser transport through tissues and have indicated that the parabolic approximation is adequate for thick tissue samples only. Also, these parabolic models have been shown not to match experimental results in other cases.[2,11,12] The commonly used parabolic model also suffers from a major drawback that it produces infinite speed of propagation of radiation transport through the medium. Monte-Carlo simulation, which includes finite speed of propagation of radiation transport, has been considered by many researchers but at a great computation expense.[5,13,14] The Monte-Carlo results also have been shown not to match the parabolic diffusion results for tissue samples of smaller thickness.[15] By an order-of-magnitude scaling analysis it can be shown that the diffusion approximation breaks down for laser pulses in the order of picoseconds or less. Also, this approximation cannot accurately account for the change in properties at internal interfaces. Therefore, analysis of time-resolved optical tomography with the goal of detection of tumors in tissues cannot be accurately performed by invoking these assumptions. Some discussions of these limitations can be found in the literature.[1,16,17] In addition, most of the previous works have not considered or have used a simplified form of scattering phase function distribution and this will lead to inaccurate transmitted and reflected signal results.

In this paper the transmitted and reflected optical signals from the tissue samples are obtained using the damped-wave hyperbolic P_1 and discrete ordinate method. Results are also obtained for the parabolic diffusion approximation in order to compare with the hyperbolic models. It is shown that the temporal shape and spread of the radiation signals obtained by the consideration of the complete transient radiative transfer equation using the discrete ordinate method are significantly different than the commonly used parabolic diffusion and hyperbolic P_1 models. This difference is particularly pronounced during the initial transients and therefore is important for analyzing data at short time scales. In addition, for the case of hyperbolic transient models it is observed that the model selected has a significant impact on the effective propagation speed of the scattered radiation fields. The effects of variation of the tissue thickness, pulse width, scattering and absorption coefficients of tissues, tumor properties and location, and scattering phase function distribution on the transmitted and reflected signals are analyzed.

2. THEORETICAL DEVELOPMENT

The physical case under consideration is a one-dimensional scattering and absorbing layered tissue medium with thickness L, infinite horizontal extent, and azimuthal symmetry. As an example, inhomogeneities such as tumors having different properties from those of the surrounding healthy tissue are present between a depth of L_1 and $L_1 + L_2$ from the tissue surface (see Fig. 1). For simplicity, the boundaries of the medium are considered to be non-reflecting and non-refracting. This geometry is chosen in order to examine the effects of various parameters with the least additional mathematical complexity. The radiative transfer equation in this geometry, assuming azimuthal symmetry and constant properties, is written as[18-20]

$$\frac{1}{c}\frac{\partial I(x,\mu,t)}{\partial t} + \mu\frac{\partial I(x,\mu,t)}{\partial x} = -\sigma_e I(x,\mu,t) + \frac{\sigma_s}{2}\int_{-1}^{1} I(x,\mu',t)\,p(\mu\rightarrow\mu')d\mu' + S(x,\mu,t) \quad , \tag{1}$$

where I is the intensity ($Wm^{-2}sr^{-1}$), c the speed of light in the medium (= speed of light in vacuum divided by the refractive index of the medium), x the Cartesian distance, t the time, σ the radiative coefficient (e, s, a refer to extinction, scattering, and absorption, respectively), μ the cosine of θ where θ is the polar angle measured from the positive x-axis (see Figure 1), p the scattering phase function and S the source term. The above is an integro-differential equation where the partial differentials represent a hyperbolic form of equation. The radiative transfer method as stated above is taken to be an accurate representation of the laser transport through tissues in the time scale of interest.

The phase function in general can be represented in terms of a series of Legendre Polynomials P_m as[21]

$$p(\Theta) = \sum_{m=0}^{M} a_m P_m(\cos\Theta) \quad , \tag{2}$$

where Θ is the scattering angle, M the order of anisotropy, and a_m are the coefficients in the expansion. For biological tissues the coefficients a_m used for the scattering phase function representation are obtained from literature[22] and is not repeated here. The advantage of this formulation is that, for the one-dimensional plane-parallel geometry and azimuthal symmetry, the phase function depends only on the initial and final values of the polar angle, as[18]

$$\frac{1}{2\pi}\int_0^{2\pi} P_m(\cos\Theta)d\varphi = P_m(\mu')P_m(\mu)\ ,\ \cos\Theta = \mu\mu' + \sqrt{1-\mu^2}\sqrt{1-\mu'^2}\cos(\varphi-\varphi') \quad , \tag{3}$$

where φ is the azimuthal angle.

The equation of transfer as given by Eq. (1) is complicated because of the integral on the right side corresponding to the in-scattering gain term. In order to reduce the integral to a simpler form, two techniques namely the linear spherical harmonics expansion (P_1) and discrete ordinate method are used in this paper. Brief outlines of these methods are discussed next.

3.1 Hyperbolic P_1 model

Under the P_1 approximation the intensity is considered to be a linear function of the direction cosine μ as follows[18,22,23]:

$$I(x,\mu,t) = u(x,t) + \frac{3}{4\pi}q(x,t)\mu \quad , \tag{4}$$

where u is the average intensity over all angles and q is the heat flux:

$$u(x,t) = \frac{1}{4\pi}\int_{4\pi} I(x,\mu,t)d\Omega = \frac{1}{2}\int_{-1}^{1} I(x,\mu,t)d\mu \quad , \tag{5}$$

$$q(x,t) = \int_{4\pi} I(x,\mu,t)\mu d\Omega = 2\pi\int_{-1}^{1} I(x,\mu,t)\mu d\mu \quad , \tag{6}$$

where Ω is the solid angle. Details about this method can be found elsewhere in the literature.[23] The resultant hyperbolic wave equation is given by[23]:

$$\frac{3}{c^2}\frac{\partial^2 u}{\partial t^2} - \frac{\partial^2 u}{\partial x^2} + \frac{3}{c}\left[\sigma_a + \sigma_e - \sigma_s\bar{p}\right]\frac{\partial u}{\partial t} + 3\left[\sigma_e - \sigma_s\bar{p}\right]\sigma_a u = \left[\sigma_e - \sigma_s\bar{p}\right]\frac{3}{2}\int_{-1}^{1} S\,d\mu - \frac{3}{2}\int_{-1}^{1}\frac{\partial S}{\partial x}\mu d\mu + \frac{3}{2}\int_{-1}^{1}\frac{1}{c}\frac{\partial S}{\partial t}d\mu \quad , \tag{7}$$

where $\bar{p}$ is an integrated phase function.[23] The above equation indicates that while propagation speed of the original laser pulse is c, the propagation speed along the x direction of the resultant hyperbolic wave of u is $c/\sqrt{3}$.

3.2 Parabolic P_1 approximation

The parabolic form of the equation, which is widely used in neutron transport[24] and has now been adopted by researchers in optical tomography applications,[25] is obtained by neglecting the first term on left-hand side and last two terms on the right-hand side of Eq. (7). It also assumes that the absorption coefficient (σ_a) is negligible compared with (σ_e - $\sigma_s\,\bar{p}$). The resulting classical diffusion equation is given by[9]

$$\frac{1}{c}\frac{\partial u}{\partial t} - \frac{1}{3(1-\bar{p})\sigma_s + \sigma_a}\frac{\partial^2 u}{\partial x^2} + \sigma_a u = \frac{1}{4\pi}\int_{4\pi} S\,d\Omega \quad . \tag{8}$$

Equation (8) implies an infinite speed of propagation of the optical signal.

3.3 Hyperbolic discrete ordinate method

The discrete ordinate method is based on a weighted, non-uniform discrete representation of the directional variation of the radiation intensity. In this method the integral on the right hand side of Eq. (1) is replaced by a quadrature, such as Gaussian, Lobatto, or Chebyshev.[26] If μ_i's are the quadrature points between the limits of integration, -1 to 1, corresponding to a 2*K* -order quadrature, and w_i's are the corresponding weights, the equation is reduced to the following system of coupled hyperbolic partial differential equations

$$\frac{1}{c}\frac{\partial I_i(x,t)}{\partial t} + \mu_i \frac{\partial I_i(x,t)}{\partial x} = -\sigma_e I_i(x,t) + \frac{\sigma_s}{2}\sum_{j=-K}^{K} w_j I_j(x,t)\, p(\mu_j \rightarrow \mu_i) + S(x,\mu_i,t)\ ,i,\ j \neq 0 \quad , \tag{9}$$

where $I_i(x,t) = I(x, \mu_i, t)$. The Gaussian quadrature of even order is used to avoid the value $\mu = 0$. The hyperbolic wave speed of I_i along the *x* direction corresponding to the discrete ordinate μ_i has the magnitude of the absolute value of $\mu_i c$.

3.4 Source pulse and boundary conditions

The pulsed radiation incident on the tissue medium is a square pulse with a temporal duration (or pulse width), t_p. The intensity in the medium can be separated into a collimated component, corresponding to the incident source, and a scattered intensity. If the collimated intensity is I_c then I is the remaining part which can be described by Eq. (1). The collimated component of the intensity, I_c, is represented by

$$I_c(x,\mu,t) = I_{incident}\exp(-\sigma_e x)[H(t-x/c) - H(t-t_p - x/c)]\,\delta(\mu - 1) \quad , \tag{10}$$

where $I_{incident}$ is the peak power at the surface, $H(t)$ the Heavyside step function and $\delta(t)$ the Dirac delta function.

The source function S for the scattered intensity field is then given by

$$S(x,\mu,t) = \frac{\sigma_s}{2}\int_{-1}^{1} I_c(x,\mu',t)\, p(\mu' \rightarrow \mu)\, d\mu' \quad . \tag{11}$$

The boundary conditions are such that the intensities pointing inward at $x = 0$ and $x = L$ are zero, yielding

$$I(x=0,\mu>0,t) = I(x=L,\mu<0,t) = 0 \quad . \tag{12}$$

The intensities at the interfaces $x = L_1$ and $x = L_2$ are assumed to be continuous.

3. RESULTS AND DISCUSSIONS

The transmitted and reflected signals are obtained numerically by solving the transient radiative transport equation given by Eq. (1). Different models used are hyperbolic discrete ordinate method, hyperbolic P_1 approximation, and parabolic diffusion approximation. For all the cases the grid sizes for both time and space variables are varied within a range of two orders of magnitude, and the results are found to be stable and converging. The optical properties considered in this paper correspond to biological tissues and tumors.[1,16] A forward peaked phase function is used to represent the tissue medium.[22]

Figures 2 and 3 show the reflected and transmitted signal for different models for a sample thickness (L) = 5 mm, scattering coefficient (σ_s) = 6.0 mm^{-1}, absorption coefficient (σ_a) = 0.012 mm^{-1}, pulse width (t_p) = 10 ps. The magnitude of transmitted and reflected signals for different models match each other only at large times. But at earlier time periods each model predicts a different temporal shape and magnitude of the transmitted and reflected signals. The hyperbolic and parabolic P_1 models give an unrealistic negative reflected signal value at small times as evident from Fig. 2 and are clearly not appropriate models for thin tissue samples.

In addition to the magnitude variation, the propagation speed of the scattered radiation is also different. It is evident from Fig. 3 that the values of the transmitted signals are zero for the hyperbolic model until the value of time taken for the exponentially decaying source pulse to traverse the medium at speed of light (c). The scattered radiation traverses the medium at a slower pace, depending upon the model selected, and therefore the earliest arriving photons correspond to those from the original laser pulse. For the P_1 model the effective signal propagation speed is $c/\sqrt{3}$ and that of the discrete ordinates method is $c\mu_i$. When higher number of ordinates is used the value of μ_i approaches unity. The discrete ordinate is expected to constitute the most accurate method because it is based on a discrete representation of the directional variation of the radiation intensity. On the other hand, the diffusion parabolic model predicts a nonzero transmission signal value even at times less than the propagation time required by the laser pulse to traverse the entire medium, which is physically impossible and is clearly evident from Fig. 3. The hyperbolic models do not suffer from such drawbacks. The hyperbolic discrete ordinate method, which is the most accurate method, is therefore used in this paper.

Figure 4 shows the transmitted signal for different sample thickness. Smaller the sample thickness higher the peak magnitude and smaller will be the temporal spread. The value of the transmitted signal is zero corresponding to the time taken by the source pulse to traverse the medium. For a 3 mm thick sample this time corresponds to 13.3 ps, for a 5 mm sample 22.2 ps, and for a 7 mm sample 31.1 ps and is demonstrated in Fig. 4. Figure 5 shows the effect of the phase function distribution on the transmitted signal. Most researchers use simple isotropic or linear forward anisotropic phase function distribution to analyze short pulse laser propagation through tissues. It is observed from Fig. 5 that the decay of the transmitted signal is much slower for isotropic and linear forward anisotropic phase function compared to the realistic highly forward anisotropic phase function for the case of tissues. The photons tend to remain inside the medium for larger times for isotropic and linear anisotropic models and thus will give incorrect transmitted signal values.

The effect of the variation of the albedo ω ($= \sigma_s / \sigma_e$) on the reflected signal is depicted in Fig. 6 by considering a multi-layered medium, i.e. tissue-inhomogeneity-tissue layer. The albedo of the tumor or inhomogeneity layer (ω_{in}) is varied whereas the albedo of the tissue medium (ω_t) is kept constant. Higher the albedo of the inhomogeneity or tumor layer, higher will be the scattering and consequently higher will be the magnitude of the reflected signals as evident from the figure. The values of the reflected signal are the same until the time taken by the laser pulse to reach the interface of tissue and inhomogeneity. The effect of the tumor location from the tissue surface is presented in Fig. 7. It is observed from the figure that as soon as the laser pulse reaches the tissue-tumor interface an inflection in the reflected signal is observed. This effect is more pronounced when the tumor is present closer to the tissue surface, i.e. for smaller L_1. Thus Fig. 7 shows that the temporal spread of the reflected signal can be used to predict the presence of tumor or inhomogeneity in the tissue medium. Figure 8 shows the effect of the laser pulse width on the reflected signal for a multi-layered medium. It is evident from the figure that shorter the laser pulse width sharper is the identity of the interface between the tissue and tumor. For 10 ps and 20 ps pulse width lasers, the inflection point corresponds to the time when the laser pulse is shut off and not to the tissue-tumor interface as in the case of 1 ps. For the case of large pulse width laser sources multiple scattering effects will smear out the sharp inflection in the reflected signal.

4. CONCLUSIONS

This paper presents results of reflected and transmitted signals for the case of short pulse laser transport through biological tissues using transient radiative transfer formulation. It is demonstrated that accurate hyperbolic discrete ordinate method should be should for such analysis rather than the commonly used parabolic diffusion approximation. The advantage of using short pulse laser probing technique is that it provides additional information about the tissue interior. The temporal spread of the reflected or transmitted signal can be correlated to the medium properties. The significance of this comprehensive study is that it will provide a guidance tool for the development of time-resolved optical tomography for biomedical imaging of tissues.

ACKNOWLEDGEMENTS

The project is sponsored by US Department of Energy, Office of Environmental and Biological Research under Contract No. DE-AC05-00OR22725 with UT Battelle, LLC. The first author (Kunal Mitra) also acknowledges partial support from Oak Ridge National Laboratory through Contract No. 4000004751.

REFERENCES

1. Y. Yamada, "Light-tissue interaction and optical imaging in biomedicine," *Annual Review of Fluid Mechanics and Heat Transfer (Ed: C.L. Tien)* **6**, pp. 1-59, 1995.

2. A. Yodh and B. Chance, "Spectroscopy and imaging with diffusing light," *Physics Today* **48**, pp. 34-40, 1995.

3. J.C. Hebden and K.S. Wong, "Time-resolved Optical Tomography," *Applied Optics* **32**, pp. 372-380, 1993.

4. R. Berg, S. Andersson-Engels, O. Jarlman, and O. Svanberg, "Time Resolved Transillumination for Medical Diagnostics," *SPIE-Time Resolved Spectroscopy and Imaging of* Tissue **1431**, pp. 110-119, 1991.

5. S.L. Jacques, "Time Resolved Propagation of Ultrashort Laser Pulses within Turbid Media," *Applied* Optics **28**, pp. 2223-2229, 1989.

6. E.A. Profio, "Light Transport in Tissue," *Applied Optics* **28**, pp. 2216-2222, 1989.

7. A. Ishimaru, "Diffusion of a Pulse in Densely Distributed Scatters," *Journal of Optical Society of America* **68**, no. 8, pp. 1045-1050, 1978.

8. D. Contini, F. Martelli, and G. Zaccanti, "Photon Migration through a Turbid Slab Described by a Model Based on Diffusion Approximation. I. Theory," *Applied Optics* **36**, pp. 4587-4599, 1997.

9. M.S. Patterson, B. Chance, and B.C. Wilson, "Time Resolved Reflectance and Transmittance for the Non-invasive Measurement of Tissue Optical Properties," *Applied* Optics **28**, pp. 2331-2336, 1989.

10. A. Ishimaru, Y. Kuga, R.L.T. Cheung, and K. Shimizu, "Scattering and Diffusion of a Beam Wave in Randomly Distributed Scatterers," *Journal of Optical Society of America* **73**, pp. 131-136, 1983.

11. A. Ishimaru, *Wave Propagation and Scattering in Random Media*, Academic Press, New York, 1978.

12. K.M. Yoo, F. Liu, and R.R. Alfano, "When Does the Diffusion Approximation Fail to Describe the Photon Transport in Random Media," *Physical Review* Letters **65**, pp. 2647-2650, 1990.

13. Y. Hasegawa, Y. Yamada, M. Tamura, and Y. Nomura, "Monte Carlo Simulations of Light Transmission through Living Tissues," *Applied* Optics **31**, pp. 4515-4520, 1991.

14. S.T. Flock, M.S. Patterson, B.C. Wilson, and D.R. Wyman, "Monte-Carlo Modeling of Light Propagation in Highly Scattering Tissues-I: Predictions and Comparison with Diffusion Theory," *IEEE Transactions on Biomedical Engineering*, **36**, pp. 1162-1168, 1989.

15. A.H. Gandbakche, R. Nossal, and R.F. Bonner, "Scaling Relationships for Theories of Anisotropic Random Walks Applied to Tissue Optics," *Applied* Optics **32**, pp. 504-516, 1993.

16. K. Mitra and S. Kumar, "Development and Comparison of Models for Light Pulse Transport Through Scattering Absorbing Media," *Applied* Optics **38**, pp. 188-196, 1999.

17. S. Kumar and K. Mitra, "Microscale Aspects of Thermal Radiation Transport and Laser Applications," *Advances in Heat* Transfer **33**, pp. 187-294, Academic Press, San Diego, 1999.

18. M.F. Modest, *Radiative Heat Transfer*, McGraw Hill, 1993.

19. M.Q. Brewster, *Thermal Radiative Transfer and Properties*, Wiley Interscience, 1992.

20. R. Siegel, and J.R. Howell, *Thermal Radiation Heat Transfer*, McGraw Hill, 1981.

21. S. Kumar and J.D. Felske, "Radiative transport in a planar media exposed to azimuthally unsymmetric incident radiation," *Journal of Quantitative Spectroscopy and Radiative Transfer* **35**, pp. 187-212, 1986.

22. M.P. Menguc and R. Viskanta, "Comparison of radiative transfer approximations for highly forward scattering planar medium," *Journal of Quantitative Spectroscopy and Radiative Transfer* **29**, pp. 381-394, 1983.

23. S. Kumar, K. Mitra, and Y. Yamada, "Hyperbolic damped-wave models for transient light pulse propagation in scattering media," *Applied Optics* **35**, pp. 3372-3378, 1996.

24. J.J. Duderstadt and L.J. Hamilton, *Nuclear Reactor Analysis*, Academic Press, New York, 1976.

25. J.C. Hebden and D.T. Delpy, "Enhanced time-resolved imaging with a diffusion model of photon transport," *Optics Letters* **19**, no. 5, pp. 311-313, 1994.

26. W.A. Fiveland, "Discrete ordinate methods for radiative transfer in isotropically and anisotropically scattering media," *Journal of Heat Transfer* **109**, pp. 809-812, 1987.

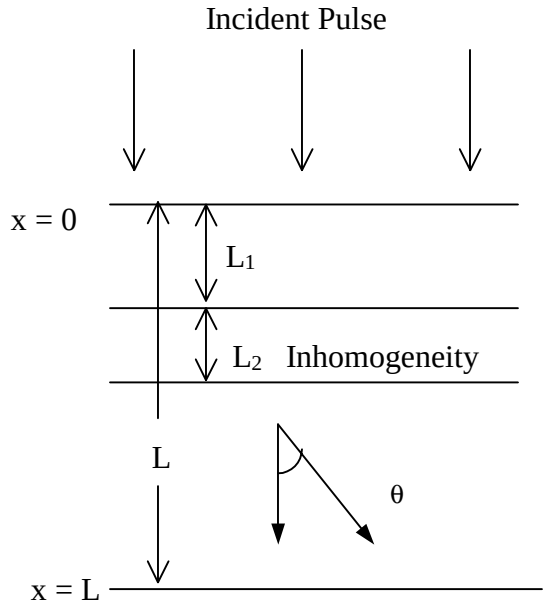

Figure 1. Schematic of the problem under consideration.

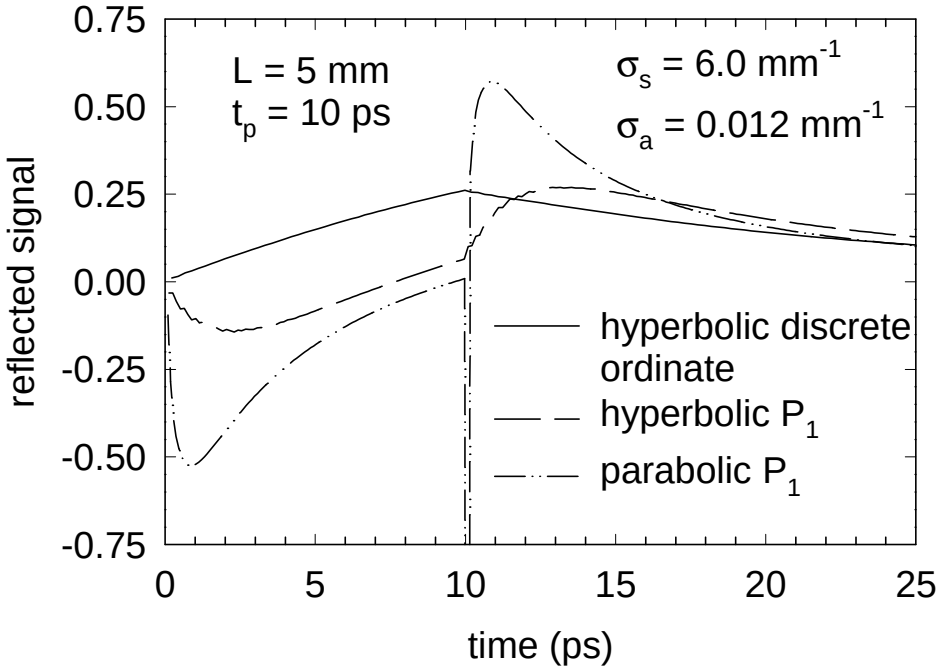

Figure 2. Reflected signal through a 5 mm tissue medium for different models.

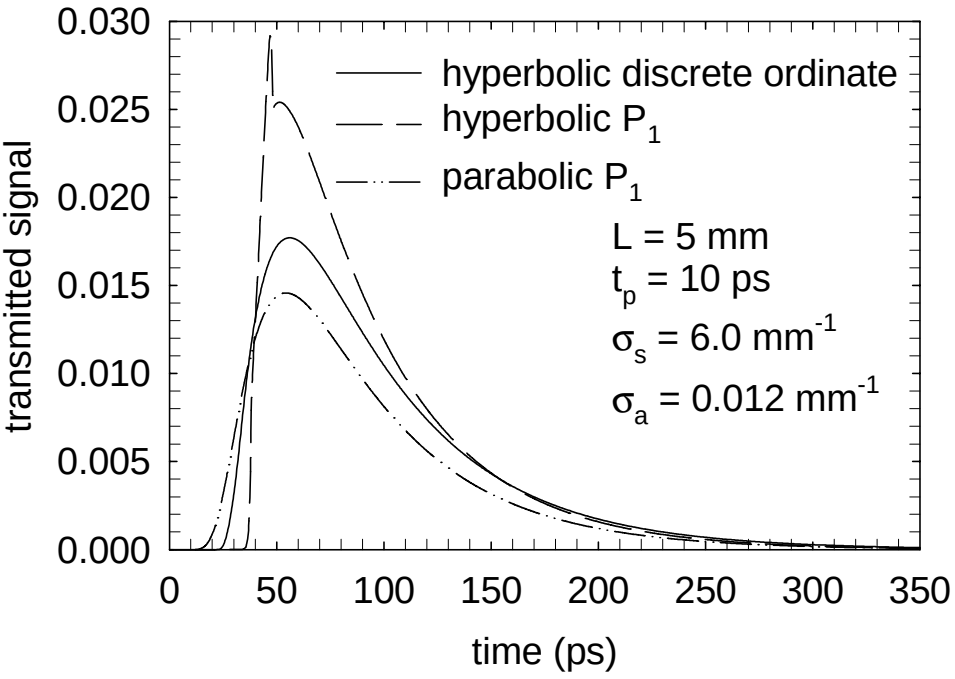

Figure 3. Transmitted signal through a 5 mm tissue medium for different models.

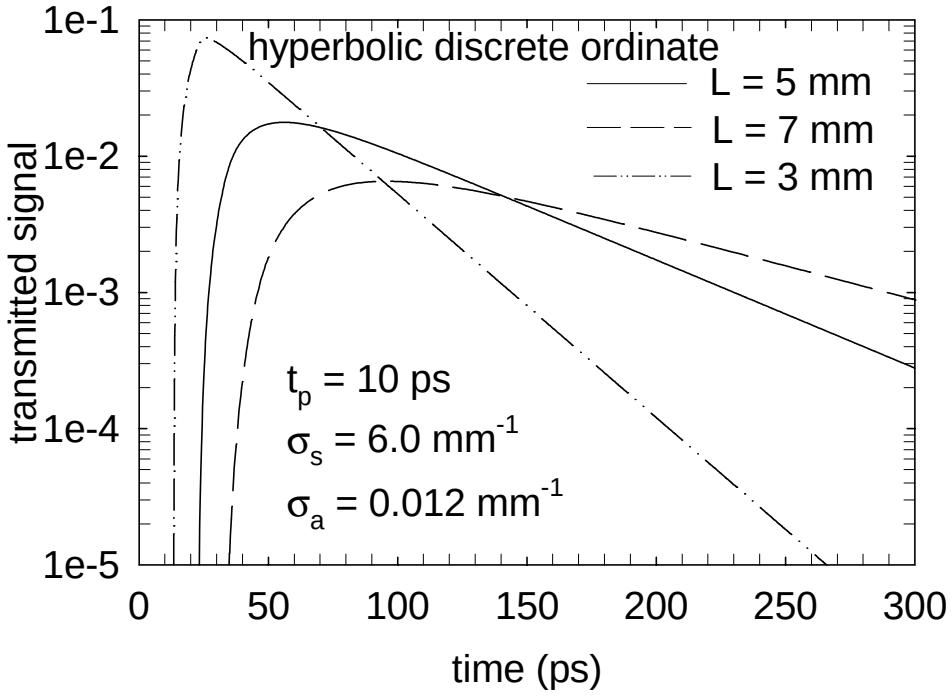

Figure 4. Transmitted signal through tissue medium of varying thickness.

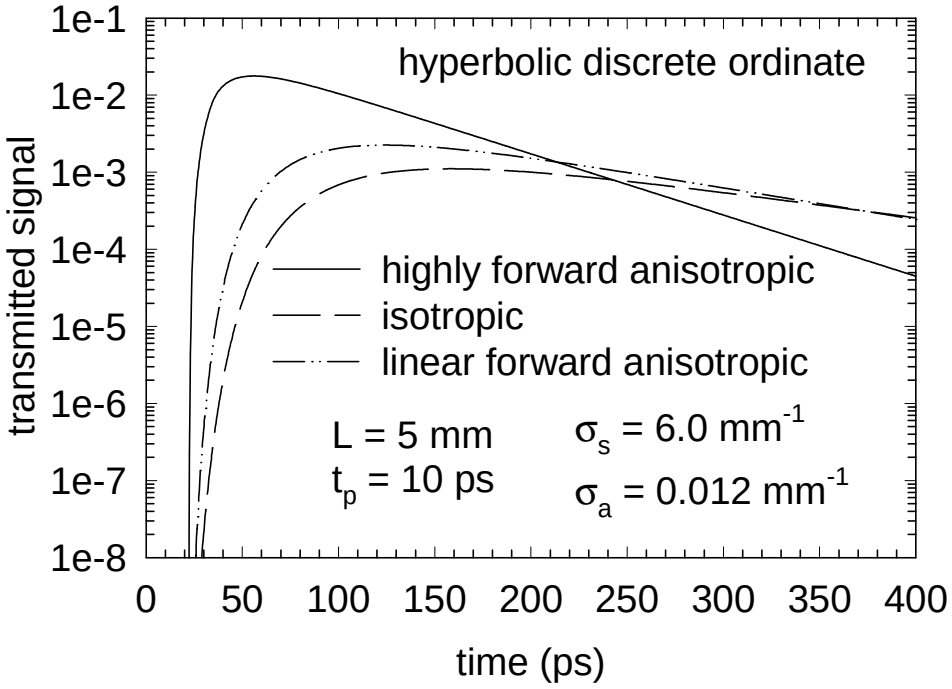

Figure 5. Transmitted signal through a 5 mm tissue medium for different phase function distribution.

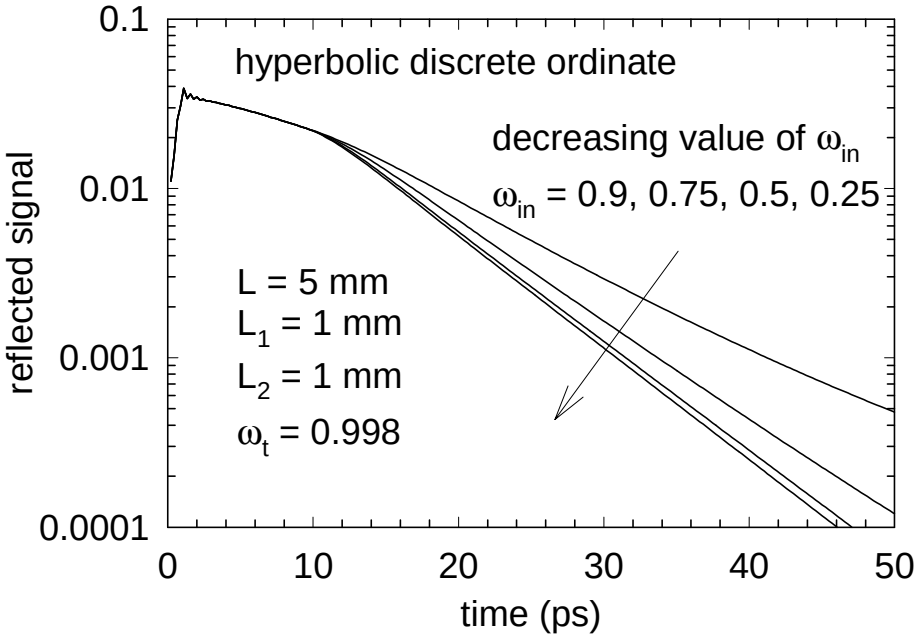

Figure 6. Reflected signal through a multi-layered medium with inhomogeneity of varying albedo imbedded in it.

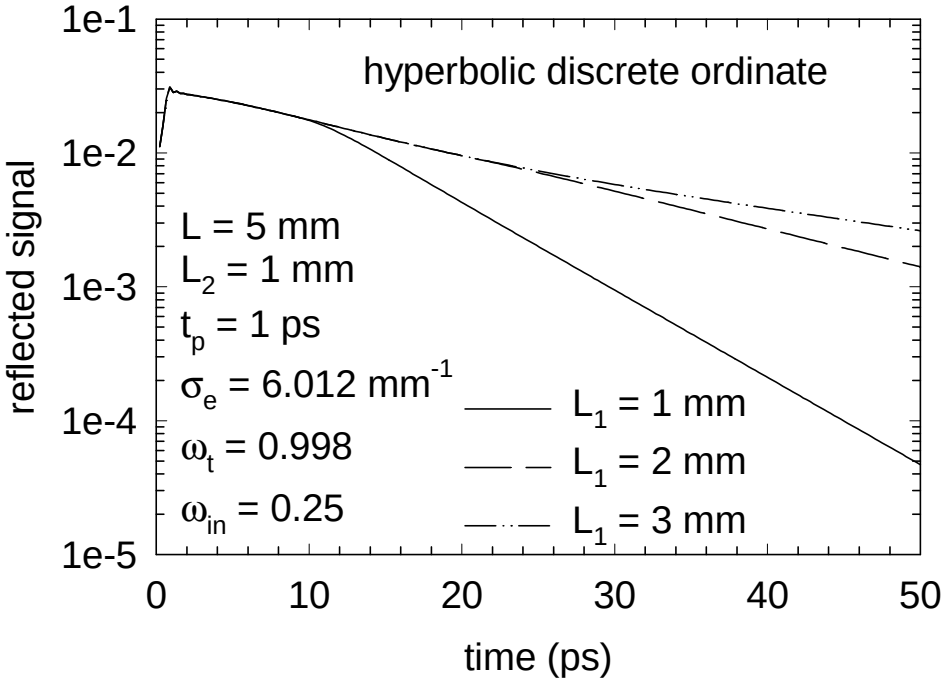

Figure 7. Reflected signal through a multi-layered medium with different inhomogeneity location from the tissue surface.

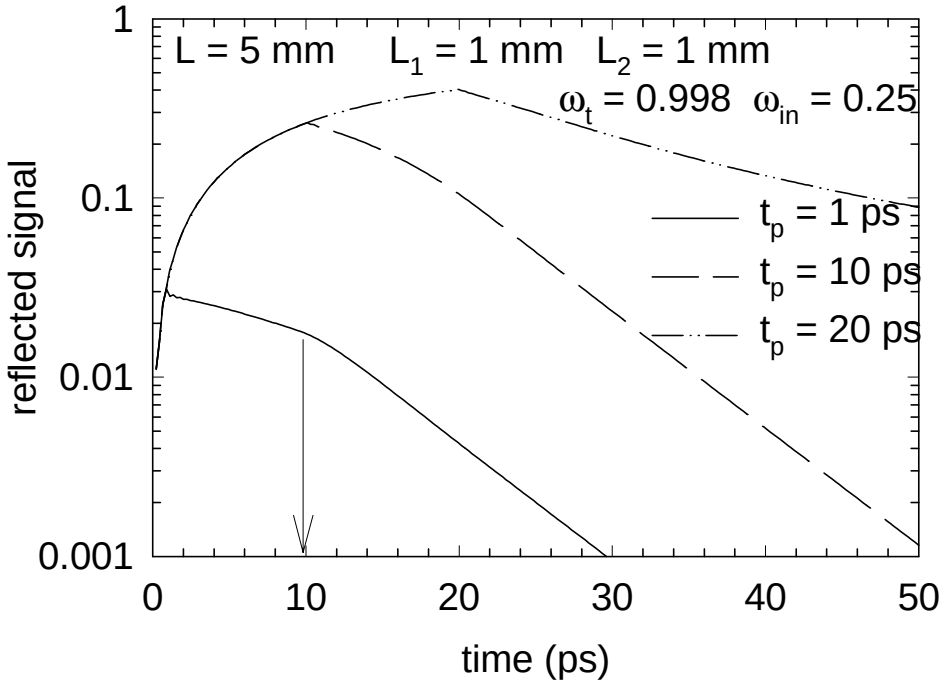

Figure 8. Reflected signal through a multi-layered medium for different laser pulse width.